Rock and Soil Mechanics

Volume 43 | Issue 12 Article 6

2-21-2023

Evaluation of cement stabilized recycled asphalt pavement/ lateritic soil blends for soft soil improvement

SUKSAN Aniroot
School of Civil Engineering, Suranaree University of Technology, Nakhon Ratchasima 30000, Thailand

HORPIBULSUK Suksun
Academy of Science, The Royal Society of Thailand, Bangkok 10300, Thailand, suksun@g.sut.ac.th

Custom Citation
SUKSAN Aniroot, HORPIBULSUK Suksun, . Evaluation of cement stabilized recycled asphalt pavement/ lateritic soil blends for soft soil improvement[J]. Rock and Soil Mechanics, 2022, 43(12): 3305-3315.

Rock and Soil Mechanics 2022 43(12): 3305–3315 ISSN 1000–7598
https: //doi.org/10.16285/j.rsm.2022.00111 rocksoilmech.researchcommons.org/journal

Evaluation of cement stabilized recycled asphalt pavement/lateritic soil blends for soft soil improvement

SUKSAN Aniroot[1], HORPIBULSUK Suksun[1, 2, 3]

1. School of Civil Engineering, Suranaree University of Technology, Nakhon Ratchasima 30000, Thailand
2. School of Civil Engineering, Center of Excellence in Innovation for Sustainable Infrastructure Development, Suranaree University of Technology, Nakhon Ratchasima 30000, Thailand
3. Academy of Science, The Royal Society of Thailand, Bangkok 10300, Thailand

Abstract: This research evaluates the potential of cement stabilized recycled asphalt pavement (RAP)/marginal lateritic soil blends as stone column aggregate instead of the traditional quarry aggregate. The undrained shear response of the blended materials at various RAP replacement ratios and effective confining pressures are investigated. The RAP replacement ratios were 10%, 30% and 50% by dry weight and ordinary Portland cement contents were 1% and 3%. It was evident that RAP replacement increased large particles and meanwhile reduced fines particles; hence the increased compactibility. Under applied effective stress lower than pre-consolidation pressure, RAP-soil blends exhibited strain-hardening behavior associated with decreased pore pressure. The strain-softening behavior in stress-strain curve for cement stabilized RAP-soil blends was diminished when RAP replacement ratio increased. The role of cementation improved the cohesion while friction angle insignificantly unchanged. The strength and stiffness of cement stabilized RAP-soil blends is mainly dependent upon the cementation bond strength and RAP replacement ratio. Shear strength improvement increased with the increased RAP replacement ratio for both unstabilized and cement stabilized RAP-soil blends while stiffness of cement stabilized RAP-soil blends decreased due to high energy absorption of asphalt binder.

Keywords: soil-cement; ground improvement; recycled asphalt pavement; triaxial; undrained behavior

1 Introduction

Stone column inclusion is a ground improvement technique to improve the impermissible soft soil layer. The main function of stone column is densifying and strengthening of the soft ground. Stone column is also used to accelerate consolidation process of soft soil. There are many installation methods of stone column for various ground condition. These installation methods form unbound backfill aggregate into the composite ground by densification.

The load capacity of the ground reinforced by stone column depends on backfill performance and confining stress[1]. Typically, the quarried stone has been selected as stone column backfill. For the past decades, the environmental impact and sustainable reasons encourage the usage of the alternative materials such as construction and demolition (C&D) materials and industrial by-products as a stone column backfill. Many researchers have ascertained the potential of the crushed concrete, steel slag and artificial cemented soil as a stone column backfill[2–5].

Installing stone columns in very soft ground (undrained shear strength <15 kPa) is not applicable due to the lack of bonding of aggregates and low shear strength of surrounding soil, causing bugling failure[1]. Stabilized aggregates with chemical agents have been applied to overcome this problem. Many researchers proposed the stabilization of fill aggregates to increase their cohesion to withstand bugling failure when installed in the soft ground[5–8].

Recycled asphalt pavement (RAP) is one of C&D materials from rehabilitation of asphalt concrete pavements. RAP is composed of aggregates and binder coating their surface[9]. The amount of RAP has been increasing annually due to the economical growth worldwide, which is generally disposed of to landfill. National Asphalt Pavement Association[10] reported that the total RAP in U.S.A. was about 101.3 million tons in 2018. The estimated 82.2 million tons of RAP were used to construct new asphalt pavements to reduce amount of natural materials. The amount of RAP used for infrastructure construction in 2018 was approximately 46.8% higher than that used in 2009.

RAP has been successfully used in highway and pavement applications[11]. Utilization of RAP in highway construction in particular base courses was achieved

Received: 3 March 2022 Revised: 20 May 2022
First author: SUKSAN Aniroot, male, born in 1989, PhD candidate, focusing on cement stabilized materials. E-mail: aniroot_suk@vu.ac.th
Corresponding author: HORPIBULSUK Suksun, male, born in 1975, PhD, Professor, mainly engaged in the research on pavement geotechnics and ground improvement. E-mail: suksun@g.sut.ac.th

by blending it with conventional aggregates (i.e., crushed rock, lateritic soil) at proper replacement ratio[12]. RAP can also improve the properties of marginal lateritic soil to meet standard specification for stabilized base course[13]. RAP-lateritic soil blends improved by cement provided the satisfactory properties for highway applications[12, 14−15].

The marginal lateritic soil, which is sub-standard for highway application but is abundant in tropical counties including Thailand can be improved by RAP to be used as a stone column backfill. For very soft Bangkok clay, the cement stabilized RAP-lateritic soil can be adopted as stone column alternative to high-quality quarry aggregate, which has an advantage in term of engineering, economic and environmental perspectives.

Therefore, this study evaluates the potential of cement stabilized RAP-marginal lateritic soil blends under compression and shear conditions. The understanding of shear response of the blended materials at various RAP replacement ratios and effective confining pressures are significant for the design of composite ground. Besides, this research outcome will be fundamental for the development of constitutive modeling for numerical simulation.

2 Materials

Lateritic soil sample was collected from a borrow pit in Nakhon Ratchasima, Thailand. The lateritic soil was composed of 15% gravel, 62% sand and 23% fine particle. Following unified soil classification system (USCS), the lateritic soil was classified as clayey sand (SC). The fine content of aggregates for highway applications must be less than 20%[16]. Therefore, this lateritic soil was classified as a marginal material, which cannot be used in highway application.

RAP was obtained from Bureau of Nakhon Ractchasima, Department of Highways, Thailand. RAP was composed of 60−70 penetration grade asphalt binder at approximately 7% by dry weight. RAP was classified as well-graded sand with gravel (SW). Basic and geotechnical properties of the lateritic soil and RAP are summarized in Table 1.

Table 1 Basic properties of lateritic soil and RAP

Materials	Liquid limit (LL) /%	Plastic limit (PL) /%	Plastic index (PI)	Gravel /%	Sand /%	Fine content /%	Specific gravity G_s	Soil classification	Asphalt binder (AS) /%
Lateritic soil	32	16	16	15	62	23	2.58	SC	—
RAP	N/A	N/A	N/A	45	43	1.4	2.35	SW	7

3 Experimental methodology

Extensive laboratory tests were conducted on cement stabilized RAP-soil blends to evaluate the effect of RAP replacement ratio and cement content on their undrained shear behavior. The lateritic soil was replaced by RAP contents at 10%, 30% and 50% by dry weight of lateritic soil to minimize the fine contents (interparticle contact prior to cement stabilization). RAP10, RAP30 and RAP50 herein represented the lateritic soil blended with 10%, 30% and 50% replacement ratio, respectively. Ordinary Portland cement (Type I) was used to stabilize RAP-soil blends at 1% and 3%(C = 1%, 3%) in this research, which is commonly used for soil stabilization in practice[17].

The compaction test was conducted on RAP-soil blends in order to determine the maximum dry density (MDD) and optimum moisture content (OMC) under modified compaction energy (ASTM D1557). Both lateritic soil and RAP were sieved through sieve No. 4 (4.75 mm) and No. 3/8 (9.5 mm), respectively to remove larger particles. The lateritic soil and RAP were air-dried for at least 3 days prior to compaction test. The lateritic soil was replaced by RAP at the target RAP replacement ratios. The RAP-lateritic soil blend was thoroughly mixed and then water was sprayed into the blend for compaction. The sample was compacted in five layers with 25 blows per layer in a standard mold with dimensions of 101.6 mm diameter and 110.68 mm height. In order to obtain complete compaction curve, at least five compaction data points were required.

The compressibility of RAP-soil samples was evaluated via one-dimensional consolidation test following ASTM D2435. The samples were prepared by tamping RAP-soil blends in three layers in a floating-type consolidation ring with dimensions of 20 mm height and 75 mm diameter at MDD and OMC. The sample was submerged under water in a consolidation cell for over 24 hours to ensure saturation before testing. The maximum effective vertical stress applied was 1 500 kPa. Due to very high yield stress of cement stabilized RAP-soil and limitation of equipment, the test was limited to only unstabilized samples.

The cement stabilized RAP-soil samples for triaxial tests were prepared by compaction method suggested by Ladd[18]. The air-dried lateritic soil, RAP and cement were thoroughly mixed by hand to attain uniform mixture prior to mixing with water at the desired quantity. The lateritic soil-RAP-cement mixture was then compacted in a steel mold with a dimension of 50 mm diameter and 100 mm height at MDD and OMC predetermined from the compaction test. After 24 hours, the samples were extruded and sealed by plastic sheet. The unstabilized samples were tested after extrusion while the cement stabilized samples were tested after 28 days of curing to avoid effect of strength development due to hydration during consolidation and shearing processes.

The undrained triaxial compression tests were conducted following the procedure suggested by Head et al.[19]. The method consists of three stages of testing namely saturation, consolidation and shearing. The saturation stage is the process allowing the water through the sample to fill the void by the incremental back pressure technique. The cell pressure and back pressure were increased while the effective stress held constant about 10 kPa until the values of Skempton B parameter reached 0.95 and 0.90 for unstabilized and cemented stabilized samples, respectively. The samples were then subjected to consolidation stage. The desired effective stresses of 50, 100 and 200 kPa were then applied on the samples until the end of consolidation. Finally, the samples were sheared with a rate of 0.1 mm /min while the back pressure valve was closed and excess pore pressure was measured during shear.

The stress-strain variants in this study were calculated as follows:

$$\left.\begin{aligned} q &= \sigma_1' - \sigma_3' \\ p' &= \frac{\sigma_1' + 2\sigma_3'}{3} \\ \varepsilon_q &= \varepsilon_a = \frac{\Delta l}{l_0} \\ \eta &= \frac{q}{p'} \end{aligned}\right\} \tag{1}$$

where σ_1', σ_2', σ_3' are effective principal stresses, q is deviator stress, p' is mean effective stress, η is stress ratio and ε_a is axial stain and ε_q is deviator strain. In the undrained condition, the volume change is not allowed, thus the shear strain and axial strain are identical.

4 Results and discussion

The particle size distribution curves of RAP-soil blends with various RAP replacement ratios are shown in Fig. 1. RAP100 and LS100 are defined as the pure RAP and pure lateritic soil. The RAP contained larger particles than the lateritic soil. The replacement of soil by RAP therefore increased the average particle size (D_{50}) of the blends and reduced fine contents.

The presence of asphalt binder with a low specific gravity of approximately 1.03 caused the RAP having lower specific gravity than the lateritic soil. The specific gravities of RAP-soil blends with different RAP replacement ratios can be approximated by using the following function:

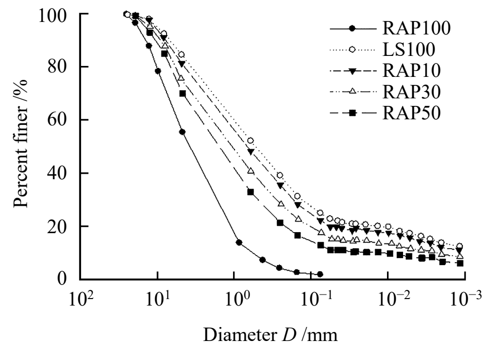

Fig. 1 Particle size distribution of RAP-soil blends

$$G_{\text{blend}} = \frac{1}{\dfrac{\text{LS}}{G_s} + \dfrac{(1-\text{LS})}{G_{\text{RAP}}}} \tag{2}$$

where G_{blend} is specific gravity of blends, G_s is specific gravity of lateritic soil, G_{RAP} is specific gravity of RAP, LS is lateritic soil content in %. The amount of asphalt binder in the blends is determined as follows:

$$A_s = \frac{W_a}{W_s} \times 100 \tag{3}$$

where W_a is weight of asphalt, W_s is weight of solid aggregates. Table 2 summarizes the calculated values of G_{blend} and A_s. The higher RAP content results in a higher asphalt binder adherence and a lower specific gravity of the blends due to lower specific gravity of RAP.

Table 2 Properties of RAP-soil blends

Sample identification	RAP /%	OMC /%	MDD /(kg • m^{-3})	Fine fraction /%	Void ratio	A_s /%
LS100	0	10.8	1 900	23	0.33	0.0
RAP10	10	10.5	1 930	21	0.29	0.7
RAP30	30	10.3	1 970	18	0.24	2.1
RAP50	50	10.3	1 970	15	0.22	3.5

4.1 Compression behavior

The results of compaction test are summarized in Fig. 2 and Table 2. The compaction curve of lateritic soil could be represented by a bell shape, typically found in granular soil. The compaction behavior of pure RAP was found to be insensitive to water (the flat compaction curve) due to high energy absorption of RAP[20]. As such, RAP alone is not suitable as the compacted fill material and must be blended with lateritic soil; the flat compaction curve of RAP tended to diminish when blended with lateritic soil. The MDD of the blends increased with increasing the RAP replacement ratio indicating the higher compactibility of the blends. The compaction curves of RAP30 and RAP50 samples were similar. The OMC of all RAP replacement ratios changed in narrow range and was approximately 10%.

The relationship between void ratio versus effective

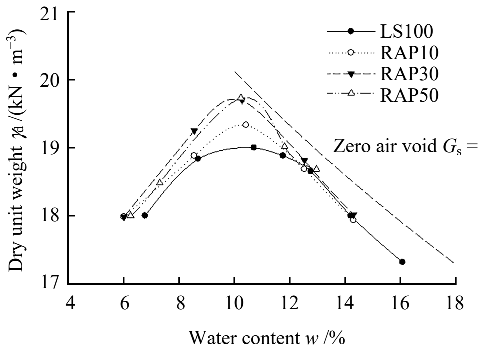

Fig. 2 Compaction characteristic of lateritic soil and RAP blends

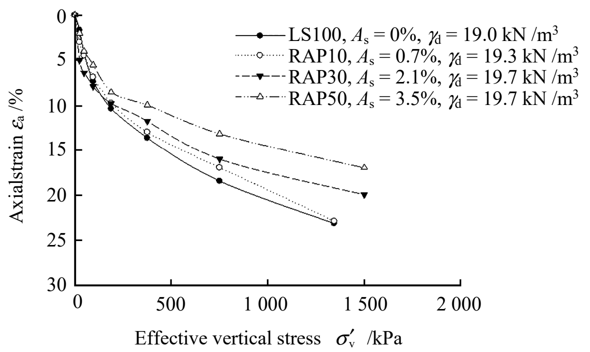

Fig. 4 Relationship between axial strain and effective vertical stress lateritic soil and RAP-soil blends

vertical stress of RAP-soil blends is shown in Fig. 3. The value of C_c reduced from 0.13 to 0.125, 0.071 and 0.076 while C_s reduced from 0.28 to 0.22, 0.16 and 0.177 for 10%, 30% and 50% RAP replacement ratios (RAP10, RAP30 and RAP50), respectively. However, RAP replacement ratio insignificantly affected the yield stress, whereby the yield stress varied between 400 and 500 kPa for all mixtures.

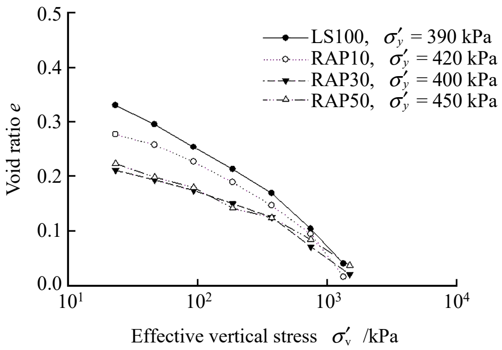

Fig. 3 Consolidation test result of RAP-soil blends

The effect of RAP replacement ratio on the deformation at the same effective vertical stress of all blends is shown in Fig. 4. At post-yield state, the lateritic soil exhibited larger deformation while the RAP50 sample exhibited the lowest deformation at the same effective vertical stress. For example, the axial strain of the RAP50 sample was 13.2% while it was 18.4% for lateritic soil at the same effective vertical stress of 750 kPa. It was noted that the RAP10 sample exhibited the similar axial strain to the lateritic soil at high stress of 1 350 kPa. The RAP replacement increased large particles and meanwhile reduced fines particles as seen by the increase of D_{50}. This improved the resistance to compression at post-yield stress as seen that even though the yield stress and density were practically the same.

4.2 Undrained shear behavior of unstabilized RAP-lateritic soil

The triaxial undrained test results of both unstabilized and stabilized samples at different RAP replacement ratios are summarized in Table 3. The undrained shear response of unstabilized lateritic soil under three confining pressures of 50, 100 and 200 kPa is presented in Fig. 5. The samples exhibited strain-hardening behavior whereby the deviator stress increased with the axial strain without clear peak. The strength and stiffness increased with the increased effective confining pressure. During shearing, the positive excess pore pressure was generated depending upon level of effective confining pressure. The higher effective confining pressure resulted in the higher excess pore pressure.

Assuming that the at-rest lateral earth pressure coefficient K_0 equals 0.5, the yield mean effective stress was calculated to be 300 kPa (the 1D yield stress was found to be 400−500 kPa from consolidation test). This yield mean effective stress was greater than the applied effective confining stresses. In other words, the samples were in over-consolidated state. Typically, over-consolidated clay exhibits negative pore pressure, which was different from the present samples. Even at low effective confining pressure of 50 kPa (the highest over-consolidation ratio, OCR), the negative pore pressure developed very little at the end of test. This might be due to the larger particles of the samples when compared with over-consolidated clay.

The undrained stress paths of unstabilized lateritic soil under 50, 100 and 200 kPa effective confining pressures are shown in Fig. 6. The path of the highest OCR samples (50 kPa of effective confining pressure) initially located close to applied total stress path due to little positive excess pore pressure development. On the other hand, the lowest OCR samples (200 kPa of effective confining pressure) moved more to the left side of the applied total stress path due to high positive excess pore pressure. However, the undrained stress paths of unstabilized lateritic soil for all effective confining pressures were turned to the right side after the peak failure was attained due to the reduction in excess pore pressure.

Table 3 Results of consolidated undrained triaxial compression test on unstabilized and cement stabilized RAP-soil blends

Samples	Cement /%	σ_c' /kPa	ε_a at q_{max} /%	ε_a at Δu_{max} /%	ε_a at η_{max} /%	q_{max} /kPa	Δu_{max} /kPa	η_{max}
LS	0	50	6.25	0.73	5.11	125.13	14.98	1.56
LS	0	100	4.59	2.35	4.16	156.26	48.41	1.46
LS	0	200	6.11	4.31	6.11	246.08	114.77	1.48
LS	1	50	6.32	0.31	0.41	523.82	24.24	2.40
LS	1	100	5.70	0.41	0.41	655.89	58.87	2.37
LS	1	200	4.79	0.62	0.83	748.40	84.34	1.94
LS	3	50	1.67	0.73	0.73	1 722.60	37.95	2.92
LS	3	100	1.56	0.45	0.51	1 875.35	53.70	2.63
LS	3	200	1.86	0.41	0.52	2 090.75	62.04	2.33
RAP10	0	50	6.20	1.14	2.31	143.70	19.14	1.56
RAP10	0	100	6.39	2.73	5.03	175.91	46.84	1.51
RAP10	0	200	6.13	4.97	4.97	265.91	107.33	1.45
RAP10	1	50	1.86	0.41	0.52	644.71	33.15	2.68
RAP10	1	100	6.32	0.52	0.62	813.41	69.01	2.49
RAP10	1	200	5.39	0.52	0.62	742.69	102.48	2.04
RAP10	3	50	1.45	0.52	0.52	1 739.53	36.88	2.91
RAP10	3	100	2.19	0.52	0.52	1 934.31	60.98	2.74
RAP10	3	200	1.46	0.63	0.73	2 192.00	139.13	2.72
RAP30	0	50	5.62	0.62	1.14	201.09	12.47	1.59
RAP30	0	100	5.04	1.26	2.42	205.07	46.30	1.52
RAP30	0	200	4.96	1.90	4.33	338.64	101.49	1.56
RAP30	1	50	7.13	0.62	0.72	835.26	32.88	2.69
RAP30	1	100	6.36	1.04	1.25	962.80	58.47	2.34
RAP30	1	200	5.44	0.84	0.94	1 042.79	117.15	2.17
RAP30	3	50	2.71	0.52	0.62	1 927.04	33.57	2.89
RAP30	3	100	1.97	0.41	0.52	2 368.55	80.75	2.89
RAP30	3	200	2.19	0.73	0.94	2 537.47	100.35	2.56
RAP50	0	50	6.31	0.84	4.21	183.55	19.40	1.73
RAP50	0	100	6.06	1.57	3.87	231.95	51.23	1.70
RAP50	0	200	6.23	3.17	6.23	424.67	95.59	1.68
RAP50	1	50	6.20	0.83	1.14	835.88	30.87	2.61
RAP50	1	100	6.38	0.84	0.94	1 000.68	70.04	2.57
RAP50	1	200	4.91	1.36	1.67	1 088.54	110.59	2.18
RAP50	3	50	3.84	0.62	0.83	1 775.99	37.95	2.92
RAP50	3	100	4.16	0.83	0.93	1 887.30	79.04	2.84
RAP50	3	200	4.16	0.62	0.73	2 381.92	144.47	2.69

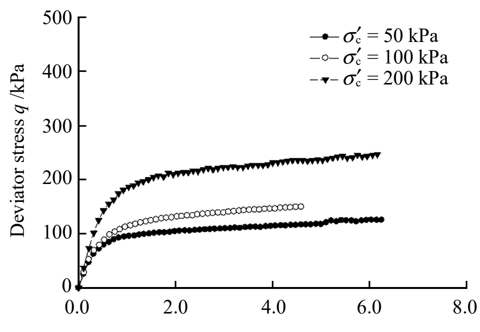

(a) Relationship of deviator stress and axial strain

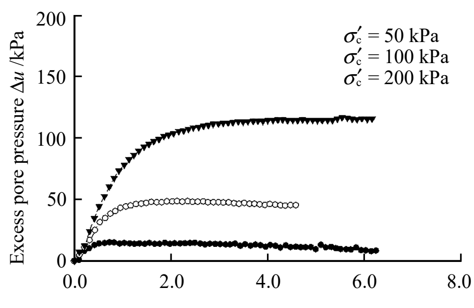

(b) Relationship of excess pore pressure and axial strain

Fig. 5 Undrained behavior of unstabilized lateritic soil

The relationship between stress ratio η versus axial strain of unstabilized lateritic soil is shown in Fig. 7. The η increased with the increased axial stain for all effective confining pressures tested but the slope of relationship was found to be different; i.e. the gentler slope was associated with the higher effective confining pressure. The maximum η was found to be identical for all the effective stresses tested, resulting in the unique failure envelope. This is the distinct undrained shear behavior of compacted lateritic soil which is different from that of normally and over-consolidated clay.

The stress versus axial strain and excess pore pressure versus axial strain relationships of unstabilized RAP-soil blends are shown Fig. 8. It is evident that the strain-hardening behavior in deviator stress versus axial stain relation is associated with the strain-softening behavior

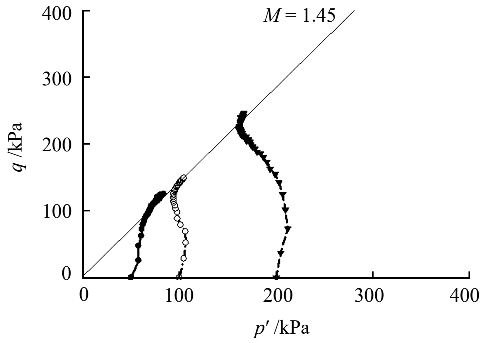

Fig. 6 The undrained stress paths of unstabilized lateritic soil

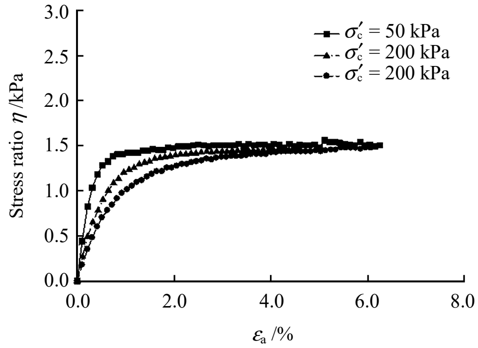

Fig. 7 Relationship between stress ratio versus axial strain of unstabilized lateritic soil

in excess pore water pressure versus axial strain relation in all RAP replacement ratios. The lower strain-softening behavior is associated with the higher effective confining pressure especially at 200 kPa. The maximum deviator stress increased with the increased RAP replacement ratio while the maximum positive excess pore pressure was more or less the same. As such, the failure envelope of RAP-soil blends was steeper than that of the unstabilized soil as shown in Fig. 9. It was evident that the cohesion c' was zero for both unstabilized soil and RAP-soil blends.

4.3 Undrained shear behavior of stabilized RAP-lateritic soil

The undrained shear behavior of cement stabilized lateritic soil at C = 1% and 3% is shown in Fig. 10. Both strength and stiffness significantly increased with increasing the cement content. For the low cement content of 1%, the cement stabilized lateritic soil sample exhibited stain-hardening behavior in deviator stress versus axial strain associated with strain-softening behavior in excess pore water pressure versus axial strain relation. However, with the high cement content of 3%, the strain-softening behavior was found for both deviator stress and excess pore pressure versus axial stain relation. The deviator stress increased to the peak at small axial stain and then decreased to lower value.

The excess pore pressure initially increased to the peak value at small stain (0.5%−1% axial strain) and then decreased to negative value. The rate of reduction in excess pore pressures depended upon degree of cementation and level of effective confining pressures. The cementation bond increased the inter-particle forces, resulting in a higher maximum deviator stress and resistance to deformation. The higher cementation bond strength was associated with the higher negative pore pressure. The strain at peak excess pore pressure was lower than that at the peak

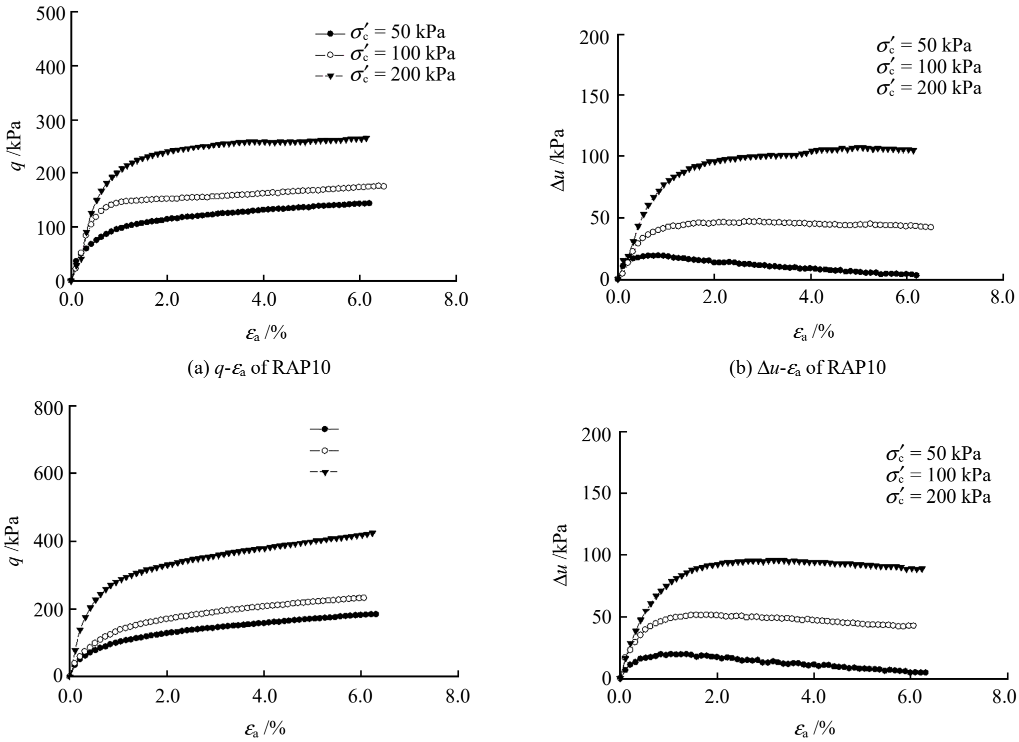

(a) q-ε_a of RAP10 (b) Δu-ε_a of RAP10

(c) q-ε_a of RAP50 (d) Δu-ε_a of RAP50

Fig. 8 Undrained behavior of unstabilized RAP10 and RAP50

DOI: 10.16285/j.rsm.2022.00111

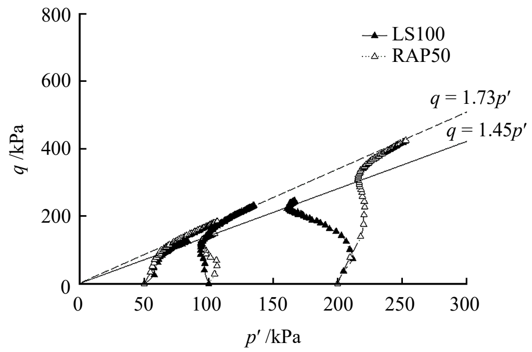

Fig. 9 Effect of RAP replacement ratio on effective stress paths of unstabilized samples

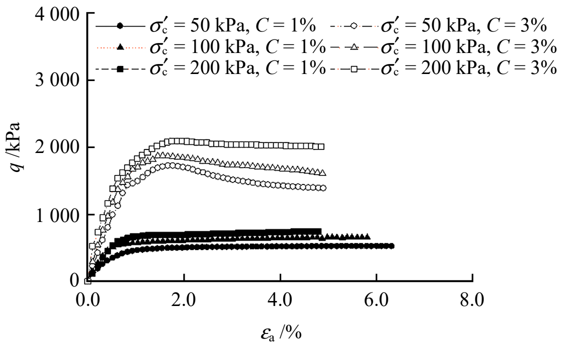

(a) q-ε_a

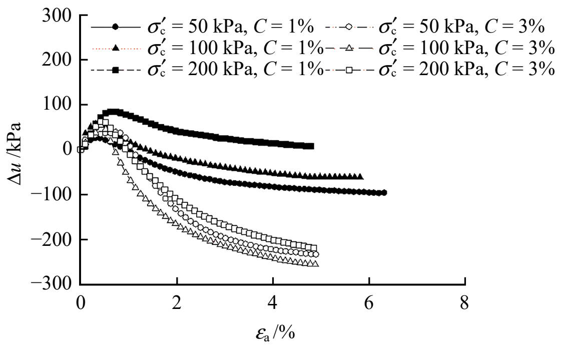

(b) Δu-ε_a

Fig. 10 Undrained behavior of cement stabilized lateritic soil

deviator stress. This is different from the cement stabilized high water content clay in that the strain at peak excess pore pressure and peak deviator stress is almost identical[21]. This difference is possibly due to the compaction energy effect, which caused the dense package

The undrained stress paths of cement stabilized lateritic soil are presented in Fig. 11. The undrained stress path finally located on the right side of applied total stress path due to negative pore pressure development. The cohesion increased with the increased cement content while the friction angle was insignificantly changed. In other words, the friction angle of cement stabilized was not significantly affected by cementation bonds. This result is in agreement with previous study reported that the friction angle of cement and unstabilized soil are identical[5, 22−23].

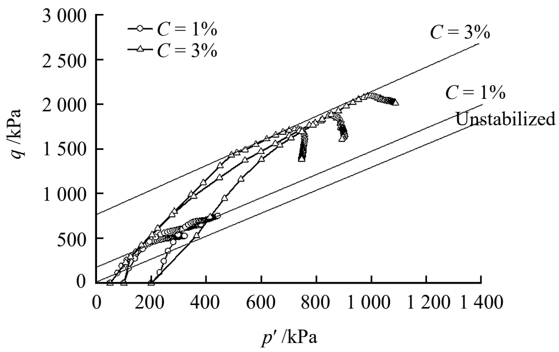

Fig. 11 Undrained stress paths of unstabilized and cement stabilized lateritic soil

The relationship between stress ratio versus axial strain of cement stabilized soil sample compared with that of unstabilized soil samples is shown in Fig. 12. The stress ratio of the stabilized samples increased to the peak at small strain after that tended to decrease to the critical state stress ratio of unstabilized samples. The higher cement content resulted in the higher peak stress ratio. It is of interest to mention that the axial strains at the peak of stress ratio were found to take place before the strain at peak deviator stress (Table 3). Coop et al.[24] revealed that the location of the breakup of the cementation bond took place at peak of stress ratio for cemented sand.

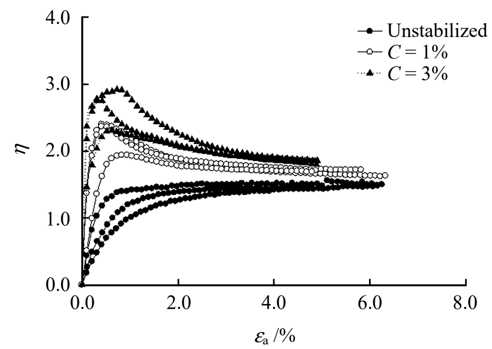

Fig. 12 Stress ratio versus axial stain relationship of unstabilized and stabilized lateritic soil samples

Horpibulsuk et al.[21] reported that the location at peak of stress ratio, peak of deviator stress and peak of excess pore pressure of cement stabilized high-water content clay was practically identical, which is different with the present study. This can be explained that the peak strength of cement stabilized lateritic soil is mainly dependent upon the cementation bond strength and interlocking due to the very low pre-shear moisture content. The cementation bond only influenced the strength until the peak of excess pore pressure.

The undrained shear behavior of cement stabilized RAP-soil blends is shown in the Fig. 13. The cement stabilized RAP-soil blends exhibited similar behavior to the cement stabilized lateritic soil. The strain-softening behavior in deviator stress and axial strain relation was

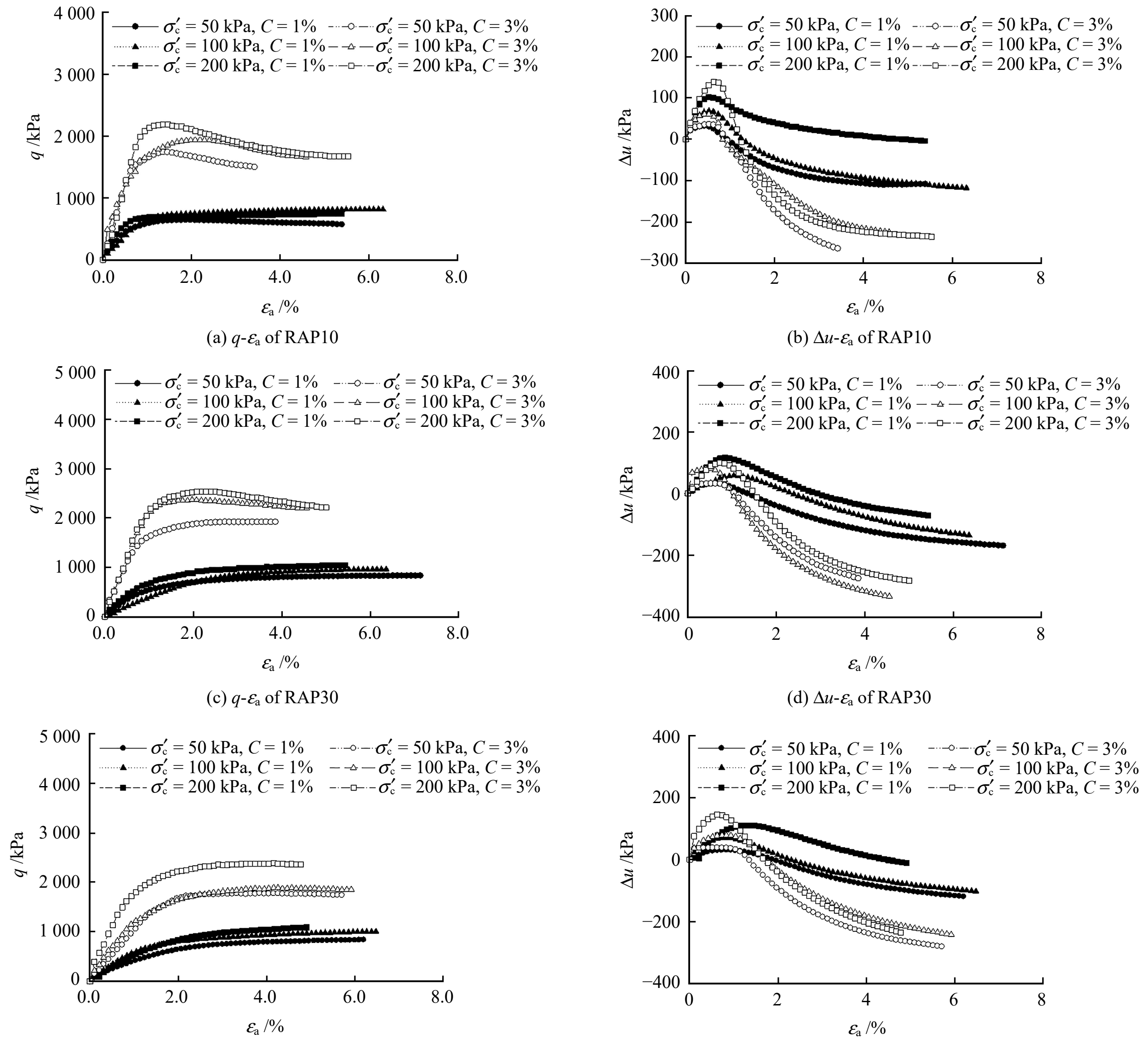

(a) q-ε_a of RAP10 (b) Δu-ε_a of RAP10

(c) q-ε_a of RAP30 (d) Δu-ε_a of RAP30

(e) q-ε_a of RAP50 (f) Δu-ε_a of RAP50

Fig. 13 Undrained behavior of cement stabilized RAP-soil blends

found for the 3% cement stabilized RAP10 and RAP30 samples whereas the cement stabilized RAP50 exhibited stain-hardening behavior in deviator stress and axial strain relation. This is because RAP50 had higher energy absorption due to higher asphalt binder in the blend. However, the cement stabilized RAP10, RAP30 and RAP50 exhibited the strain-softening behavior in excess pore pressure and axial strain relation. In other words, the asphalt binder content did not affect the excess pore pressure development. Similar to the cement stabilized lateritic soil, the peak positive excess pore pressure took place at small stain, which was also observed for cement stabilized RAP-soil blends.

4.4 Strength and ductility improvement due to RAP replacement

The effect of RAP replacement ratio on shear strength improvement Δq is determined as follows:

$$\Delta q = q_R - q_s \tag{4}$$

where q_R is the deviator stress of RAP-soil blends samples and q_s is the deviator stress of the lateritic soil at the same axial strain level in similar test conditions. The relationship of Δq versus axial strain of both unstabilized and cement stabilized RAP-lateritic soil samples under 200 kPa confining pressure is shown in Fig. 14. For unstabilized samples, Δq was higher for higher RAP replacement ratio because the increased RAP replacement ratio caused denser particle package and lower void ratio. For low cement content of 1%, except RAP10 sample, Δq decreased initially to the lowest value and then increased sharply to the peak value before levelling off.

The decrease of Δq at the initial stage is because the slope of stress-stain curve of cement stabilized RAP-soil blends was lower than that of cement stabilized lateritic soil. In other words, the gentle strength development at the initial stage was found for RAP10 while the significant

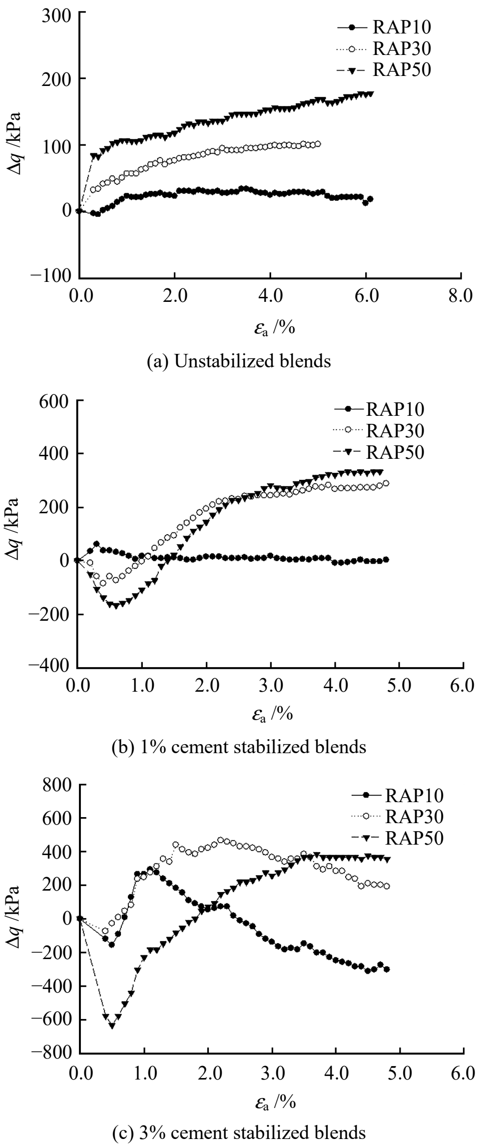

Fig. 14 Strength improvement under 200 kPa confining pressure

strength development associated with lower stiffness was found for RAP30 and RAP50 samples. The shear strength improvement at larger strain was more with the increased RAP replacement ratio for both the unstabilized and stabilized RAP-soil samples. With strain-softening behavior in deviator stress and axial strain relation for 3% cement samples, Δq of RAP10 and RAP30 samples decreased after the peak value. On the other hand, Δq of RAP50 sample increased gradually even with the increase in strain due to strain-hardening behavior. It is clear that Δq increased with the increased RAP replacement ratio for both unstabilized and cement stabilized RAP-soil blends. Due to high energy absorption of asphalt binder, the more delay in Δq of cement stabilized RAP-soil blends was found at initial stage as the RAP replacement ratio increased. Eventually, the strength development of cement stabilized RAP-soil was mobilized at larger strain due to interlocking.

The variation in shear improvement as discussed early indicated the lower slope of stress-stain curve of cement stabilized samples when RAP replacement ratio increased. To evaluate the effect of RAP replacement on stiffness of cement stabilized RAP-soil blends, the initial tangent modulus E_i of the blends with various RAP replacement ratios and cement contents was compared. The E_i of stabilized materials is typically steeper with an increase of confining pressure. The normalized initial tangent modulus by atmosphere pressure (P_a = 101.3 kPa) is employed to evaluate the stiffness of the cement stabilized RAP-soil blends. The relationship between E_i versus confining pressure normalized by P_a in log-log scale is shown Fig. 15 and can be expressed in term of power function[25] as follows:

$$E_i = kP_a\left(\frac{\sigma_c'}{P_a}\right)^n \qquad (5)$$

where k is the intercept at $\frac{\sigma_c'}{P_a}=1$ and n is slope.

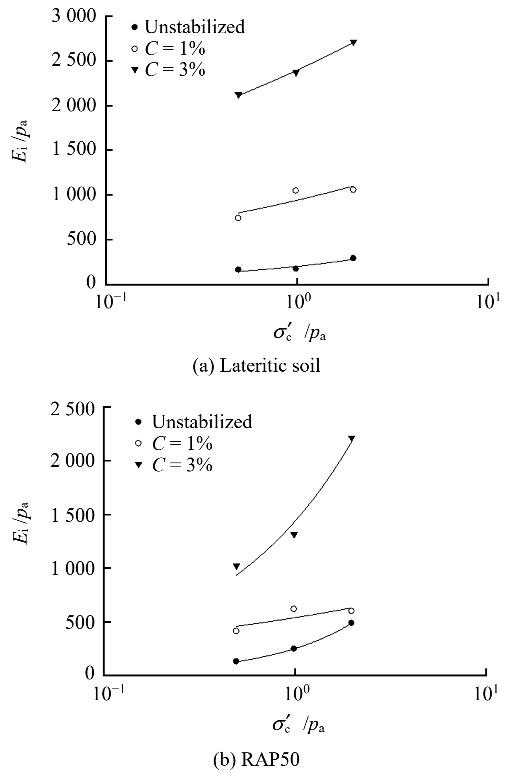

Fig. 15 Normalized initial stiffness versus normalized effective confining pressure

Table 4 summarizes the result of E_i for unstabilized and cement stabilized RAP-soil blends. The relationship of the coefficient of k versus RAP replacement ratios is shown in Fig. 16. As expected, k of unstabilized samples gradually increased with RAP replacement ratio associated with the increased shear improvement. With higher cement content, at the same RAP replacement ratio, k increased because the higher cementation bond strength induced more resistance to deformation during shear (higher slope stress-strain curve).

The increase of k value with cement content is in agreement with the result of cement stabilized sand reported by previous studies[26−27]. However, k of cement stabilized RAP-soil blends decreased with the increased RAP replacement ratio. Hoy et al.[28] investigated the microstructure of RAP using scanning electron microscope and indicated that asphalt binder partly coated the surface of aggregate and hence resulted in lower stiffness.

Table 4 Values of stiffness parameter

Sample name	RAP content /%	Cement C /%	k	n
LS100	0	0	201.14	0.418 1
		1	975.26	0.258 1
		3	2 397.10	0.176 7
RAP10	10	0	229.56	0.445 0
		1	945.07	0.237 8
		3	2 922.90	0.231 0
RAP30	30	0	247.98	0.675 3
		1	611.50	0.148 1
		3	2 315.40	0.124 0
RAP50	50	0	219.80	0.967 9
		1	534.89	0.267 7
		3	1 405.00	0.568 7

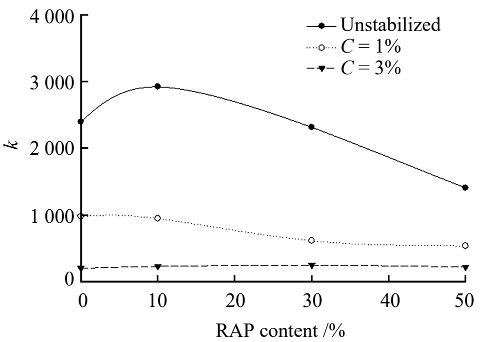

Fig. 16 Effect of RAP on k value

In this research, the role of cementation bonds and compaction energy on the undrained shear response of cement stabilized RAP-lateritic soil was illustrated. Due to the break-up of cementation bonds, the strain-softening in both deviator stress-axial strain and excess pore pressure-axial strain is detected. The RAP replacement was found to prevent the sudden break-up of the cementation bonds as seen by the smaller reduction in deviator stress after the peak state with a higher RAP replacement ratio. The understanding of the different shear responses of this material in stabilized and unstabilized states is vital for development of constitutive models based on the soil structure concept such as Structured Cam Clay model[29−33].

The stabilized RAP-lateritic soil can be used as the stone columns in soft Bangkok clay whose undrained shear strength is low. The apparent cohesion of the RAP-lateritic soil can reduce the lateral earth pressure, which prevents the failure of the surrounding clay during the installation of RAP-lateritic soil. The RAP replacement can improve the ductility of the composite ground during the service state especially under cyclic and earthquake conditions.

5 Conclusions

This research evaluates the undrained shear response of cement stabilized recycled asphalt pavement/marginal lateritic soil blends at various RAP replacement ratios and effective confining pressures. The RAP replacement improved the gradation and maximum dry density of lateritic soil; hence the resistance to compression at post-yield stress. The unstabilized RAP-soil blends exhibited strain-hardening behavior in deviator stress versus axial stain relation associated strain-softening behavior in excess pore water pressure versus axial strain relation.

For cement stabilized RAP-soil blends at low cement of 1%, RAP-soil blends exhibited stain-hardening behavior in deviator stress versus axial strain. But with the high cement content of 3%, the strain-softening behavior was found for both deviator stress and excess pore pressure versus axial stain relation. The high RAP replacement ratio of 50% can prevent the strain softening in deviator stress versus axial stain relation due to high energy absorption of asphalt.

The failure envelope of unstabilized RAP-soil blends was steeper with the increased RAP replacement ratio while the cohesion c' was zero. For cement stabilized samples, the undrained stress paths located the right side of applied stress path total stress path due to negative pore pressure development. The cohesion increased with the increased cement content while the friction angle was insignificantly changed.

The RAP replacement was found to improve the shear strength in both unstabilized and stabilized states. Due to high energy absorption of asphalt binder, the higher RAP replacement led to a more delay in shear strength improvement but a lower initial stiffness (more ductile behavior) of cement stabilized RAP-soil blends.

References

[1] HAN J. Principles and practice of ground improvement[M]. Hoboken, New Jersey: John Wiley & Sons, Inc., 2015.

[2] MCKELVEY D, SIVAKUMAR V, BELL A, et al. Shear strength of recycled construction materials intended for use in vibro ground improvement[J]. Ground Improvement, 2002, 6(2): 59−68.

[3] SHAHVERDI M, HADDAD A. Use of recycled materials in floating stone columns[C]//Proceedings of the Institution of Civil Engineers - Construction Materials. [S. l.]: [s. n.],

2019.

[4] ZUKRI A, NAZIR R. Sustainable materials used as stone column filler: a short review[C]//IOP Conference Series: Materials Science and Engineering. [S. l.]: [s. n.], 2018.

[5] JURAN I, RICCOBONO O. Reinforcong soft soil with artificially cemented compacted-sand column[J]. Journal of Geotechnical Engineering, 1991, 117(7): 1042−1060.

[6] GOLAIT Y S, PADADE A H. Analytical and experimental studies on cemented stone columns for soft clay ground improvement[J]. International Journal of Geomechanics, 2017, 17(4): 0401616100.

[7] GOLAIT Y S, SATYANARAYANA V, RAJU S S V. Concept of under rammed cemented stone column for soft clay ground improvement[C]//Indian Geotechnical Conference. Mumbai, India: [s. n.], 2009: 356−360.

[8] ZHOU C, YIN J H, MING J P. Bearing capacity and settlement of weak fly ash ground improved using lime – fly ash or stone columns[J]. Canadian Geotechnical Journal, 2002, 39(3): 585−596.

[9] CHESNER W H, COLLINS R J, MACKAY M H. User guidelines for byproducts and secondary use materials in pavement construction[M]. McLean, VA: Federal Highway Administration, 2008.

[10] National Asphalt Pavement Association. 9th Annual Asphalt Pavement Industry Survey, IS-138 Appendix B: State-by-State Use of Recycled Materials and Warm-Mix Asphalt In Asphalt Pavement Mixtures[M]. Greenbelt, MD: NAPA, 2019.

[11] BENNERT T, PAPP M, MAHER A, et al. Utilization of construction and demolition debris under traffic-type loading in base and subbase applications[J]. Transportation Research Record: Journal of the Transportation Research Board, 2000, 1714(1): 33−39.

[12] TAHA R, AL-HARTHY A S, AL-SHAMSI K, et al. Cement stabilization of reclaimed asphalt pavement aggregate for road bases and subbases[J]. Journal of Masterials in Civil Engineering, 2002, 14(3): 239−245.

[13] SUEBSUK J, HORPIBULSUK S, SUKSAN A, et al. Strength prediction of cement-stabilised reclaimed asphalt pavement and lateritic soil blends[J]. International Journal of Pavement Engineering, 2017: 332−338.

[14] SUEBSUK J, SUKSAN A, HORPIBULSUK S. Strength assessment of cement treaded soil-reclaimed asphalt pavement (RAP) mixture[J]. International Journal of GEOMATE, 2014, 6(2): 878−884.

[15] GUTHRIE W S, COOLEY D, EGGETT D L. Effects of reclaimed asphalt pavement on mechanical properties of base materials[J]. Journal of the Transportation Research Board, 2007, 2005: 44−52.

[16] Department of Highway. DH-S 205/1989 Strand for of base course aggregate Thailand[S]. Bangkok: Department of Highway, 1989.

[17] HORPIBULSUK S, KATKAN W, SIRILERDWATTANA W, et al. Strength development in cement stabilized low plasticity and coarse grained soils: laboratory and field study[J]. Soils and Foundations, 2006, 46(3): 351−366.

[18] LADD R S. Preparing test specimens using undercompaction[J]. Geotechnical Testing Journal, 1978, 1(1): 16−23.

[19] HEAD K H, EPPS R J. Manual of soil laboratory testing: effective stress tests[M]. Dunbeath: Whittles Publishing, 2014.

[20] ARULRAJAH A, DISFANI M M, HORPIBULSUK S, et al. Physical properties and shear strength responses of recycled construction and demolition materials in unbound pavement base/subbase applications[J]. Construction and Building Materials, 2014, 58: 245−257.

[21] HORPIBULSUK S, MIURA N, BERGADO D T. Undrained shear behavior of cement admixed clay at high water content[J]. Journal of Geotechnical and Geoenvironmental Engineering, 2004, 130(10): 1096−1105.

[22] CLOUGH G W, SITRA N, BACHUS R C. Cemented sand under static loading[J]. Journal of the Geotechnical Engineering Division, 1981, 100(6): 799−817.

[23] SCHNAID F, PRIETTO P D M, CONSOLI N C. Chaeacterization of cemented sand in triaxial compression[J]. Journal of Geotechnical and Geoenvironmental Engineering, 2001, 127(10): 857−868.

[24] COOP M R, ATKINSON J H. The mechanics of cemented carbonate sands[J]. Geotechnique, 1993, 43(1): 53−67.

[25] JANBU N. Soil compressibility as determined by oedometer and triaxial test[C]//Proceedings of European Conference on Soil Mechanics and Foundation Engineering (ECSMFE). Wiesbaden: [s. n.], 1963: 19−25.

[26] SCHNAID F, PRIETTO P D M, CONSOLI N C. Characterization of cemented sand in triaxial compression[J]. Journal of Geotechnical and Geoenvironmental Engineering, 2001, 127(10): 857−868.

[27] CLOUGH G W, SITAR N, BACHUS R C, et al. Cemented sands under static loading[J]. Journal of the Geotechnical Engineering Division, 1981, 107(6): 799−817.

[28] HOY M, HORPIBULSUK S, ARULRAJAH A. Strength development of recycled asphalt pavement – fly ash geopolymer as a road construction material[J]. Construction and Building Materials, 2016, 117: 209−219.

[29] HORPIBULSUK S, LIU M D, LIYANAPATHIRANA D S, et al. Behavior of cemented clay simulated via the theoretical framework of the Structured Cam Clay model[J]. Computers and Geotechnics, 2010, 37: 1−9.

[30] SUEBSUK J, HORPIBULSUK S, LIU M D. Modified structured Cam Clay: a constitutive model for destructured, naturally structured and artificially structured clays[J]. Computers and Geotechnics, 2010, 37: 956−968.

[31] SUEBSUK J, HORPIBULSUK S, LIU M D. A critical state model for overconsolidated structured clays[J]. Computers and Geotechnics, 2011, 38(5): 648−658.

[32] SUEBSUK J, HORPIBULSUK S, LIU M D. Finite element analysis of the non-uniform behavior of structured clay under shear[J]. KSCE Journal of Civil Engineering, 2016, 20(4): 1300−1313.

[33] SUEBSUK J, HORPIBULSUK S, LIU M D. Compression and shear responses of structured clays during subyielding[J]. Geomechanics and Engineering, 2019, 18(2): 121−131.